Supporting Information:

Substrate Integrated Nickel-Iron Ultra-Battery with Extraordinarily Enhanced Performances

*Debasish Sarkar, Ashok Shukla and D. D. Sarma**[1]

Solid state and Structural Chemistry Unit, Indian Institute of Science, Bengaluru-560012, India.

AUTHOR INFORMATION

***Corresponding Author:** E-mail: sarma@sscu.iisc.ernet.in

[1]Also at Jawaharlal Nehru Centre for Advanced Scientific Research, Bengaluru- 560054, India, and Department of Physics and Astronomy, Uppsala University, Box-516, SE- 75120, Uppsala, Sweden.

Calculations for Capacity, energy and power:

For single electrode and cell measurements:

Specific capacity (C_{sp}) is calculated from the cyclic voltammogram data using the equation:

$$C_{sp} = \int idt / m ,$$

where, i is the cathodic or anodic current, dt is the time differential and m is the mass of the redox active materials.

Areal capacitances (C_a) and specific capacitance (C_s) for the electrodes are calculated using equations:

$$C_a = \frac{\int idt}{A\Delta V} \text{ and, } C_s = \frac{\int idt}{m\Delta V} ,$$

with A and ΔV be the area of the electrode and potential window, respectively.

Specific capacity (C_s) values are calculated from discharge data for the electrodes using the equation:

$$C_s = i\Delta t / m ,$$

where, i is the discharge current, Δt is the discharge time and m is the mass of the active materials.

Gravimetric energy (W) and power densities (P) for the fabricated cell are calculated using equations:

$$W = \int i\Delta V dt / m$$

and

$$P = W / \Delta t ,$$

where, i is the discharge current, Δt is the discharge time for the discharge voltage ΔV, dt is the time differential and m is the total mass of the active materials (α-Fe_2O_3 and NiO both).

Physical and electrochemical characterization

Morphology, structure and composition of different nano-structures were investigated using field emission SEM (FESEM, FEI, Quanta FEG 650), TEM (TEM, JEOL JEM-2100F) and XRD (XRD, PANalytical Empyrean X-ray Diffractometer). X-ray absorption near edge structure (XANES) at the O *K*-edge, Fe *L*-edge and Ni *L*-edge were obtained by I1011 beam line at the Max II storage ring, in the Max Lab Synchrotron Radiation Laboratory and were recorded in surface sensitive total electron (TEY) mode.

All electrochemical characterizations on the as prepared samples were carried out using a software-controlled conventional three-electrode electrochemical cell (AutoLab PGSTAT 302N) comprising the as prepared samples (1×1 cm^2 in size) as working electrodes, a Pt foil as counter electrode and Hg/HgO (MMO) as reference electrode in 1M aqueous KOH solution, at room temperature (25^{o}C). Electrochemical performance of the assembled ultra-battery was investigated in 2-electrode configuration with reference and counter electrode shorted.

The pictorial details for individual electrodes and assembled cell are given below.

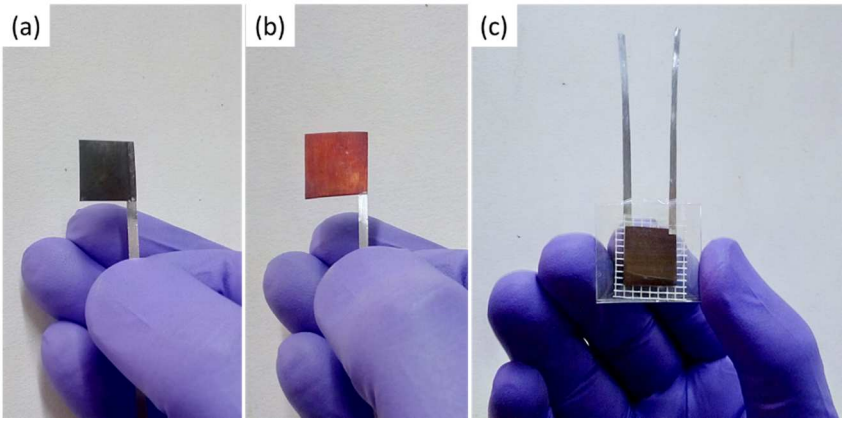

Figure S1. Pictorial details for (a) NiO positive electrode, (b) α-Fe_2O_3 negative electrode and (c) NiO//α-Fe_2O_3 2-electrode prototype cell.

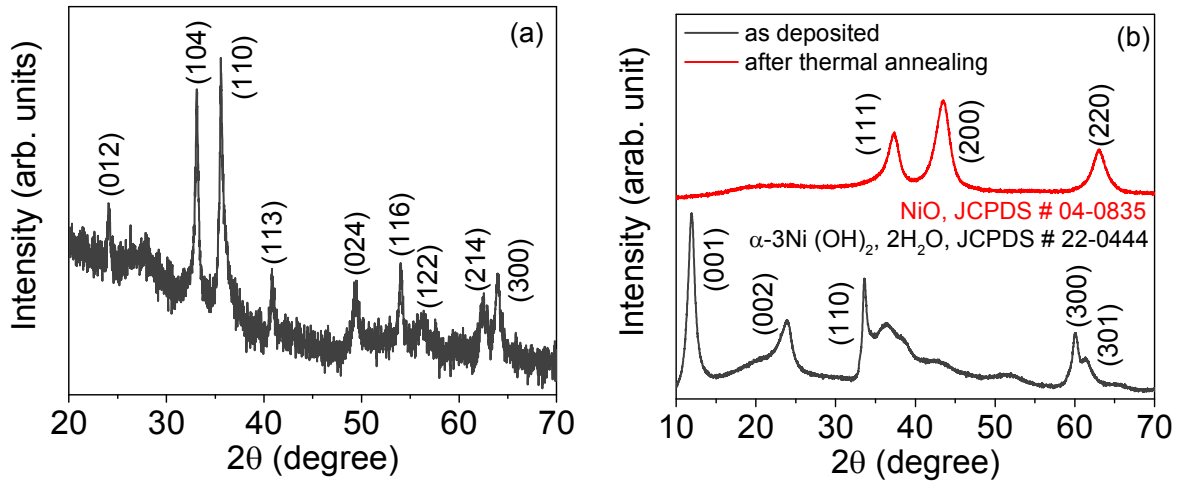

Figure S2. XRD patterns of the samples deposited on the SS substrate, (a) for α-Fe_2O_3 nano-rods and (b) for NiO nano-flakes.

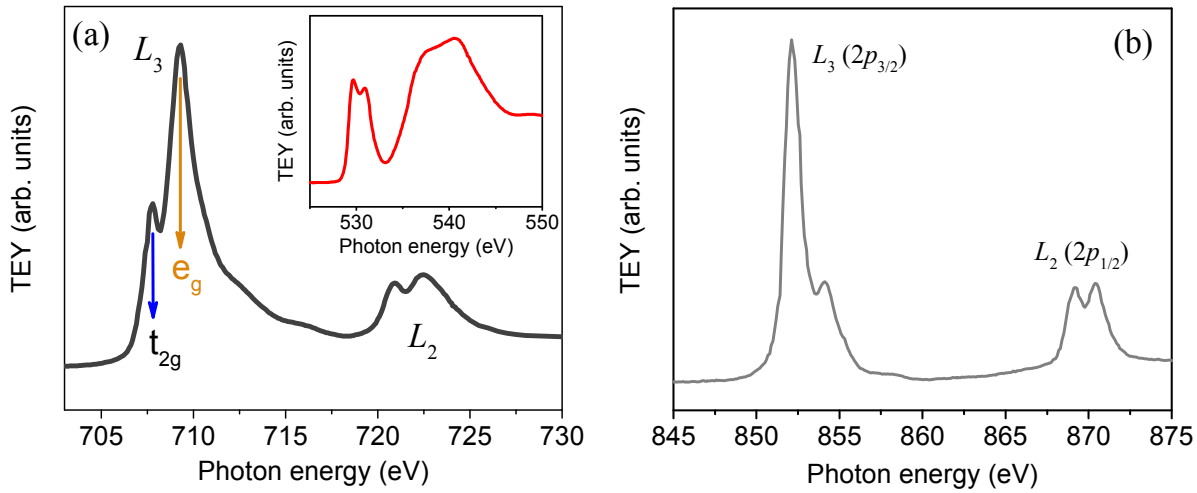

Figure S3. (a) Fe L-edge XANES spectra recorded in total electron yield (TEY) mode for α-Fe_2O_3 nano-rods, inset graph shows the corresponding O K-edge spectra. (b) provides Ni L-edge XANES spectra of the NiO nano-flakes.

Figure S3a shows the X-ray Absorption Near Edge Structure (XANES) for the Fe *L*-edge, shape that appears to be similar to the XAS measurements on single crystalline and poly-crystalline α-Fe_2O_3 samples.[1-3] In the spectra, the L_3 and L_2-edges, located at nearly 710 and 721 eV, respectively, correspond to the electron transfer from a Fe (2*p*) state to an unoccupied Fe (3*d*) orbital; Fe($2p_{3/2}$) – 3(*d*) for L_3 and Fe($2p_{1/2}$) – 3(*d*) for L_2 edges. Here, the distinct ligand field splitting of the L_3-edge suggests the presence of only Fe^{3+} valence state of iron.[3] However, in the normalized XANES spectra for O *K*-edge (Figure S3a, inset), the first edge, centered at ~ 530 eV, splits into Fe 3*d* t_{2g} and Fe 3*d* e_g states, due to the electron transfer from O1(*s*) state to the hybridized O(2*p*) – Fe(3*d*) states whereas the higher energy edge after 535 eV corresponds to the O(2*p*) states hybridized with Fe (4*s*, 4*p*) states.[3]

In this case also, XAS measurements were performed to confirm the chemical state of Ni in NiO nano-flakes and the corresponding Ni *L*-edge XANES spectra is depicted in Figure S3b. As can be seen, the Ni *L*-edge XANES spectra shows two strong absorption features due to the spin-orbit splitting of the Ni 2*p* core hole, namely L_2 ($2p_{1/2}$) and L_3 ($2p_{3/2}$) edges in between 868 and 872 eV and 853 and 857 eV, respectively.[4] The shape of the Ni *L*-edge XANES spectra is in good agreement with that reported by Van der Laan et al. for NiO, suggesting the presence of only Ni^{2+} high-spin state of the Ni ions in the oxide nano-flakes sample with no evidence of the presence of either divalent Ni^{2+} low-spin or trivalent Ni^{3+} states.[4,5]

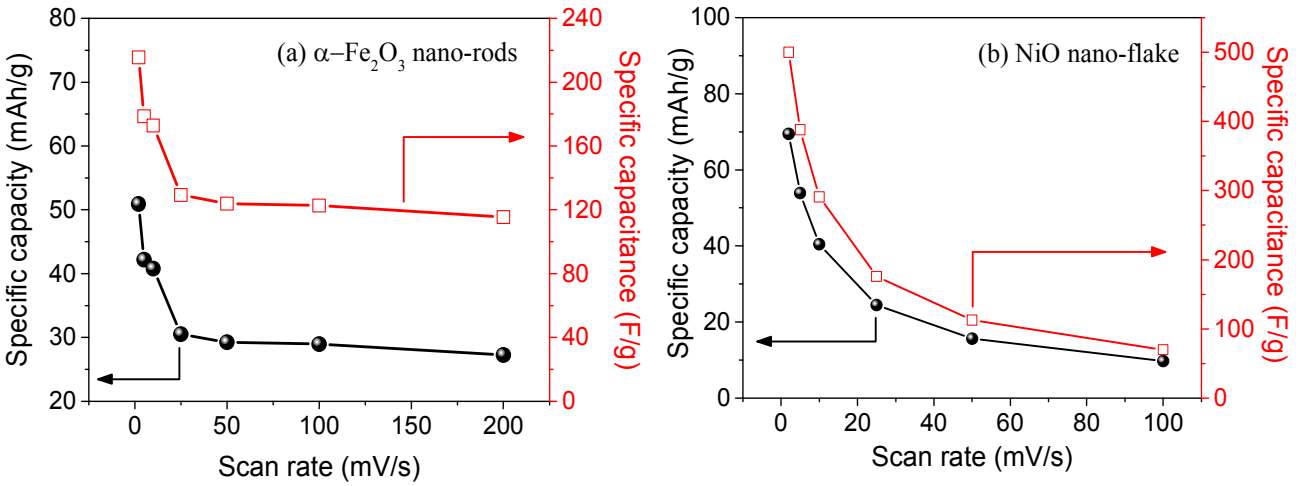

Figure S4. Variation of specific capacity and capacitance with potential scan rates for α-Fe_2O_3 nano-rod negative electrode material (a) and NiO nano-flake positive electrode material (b).

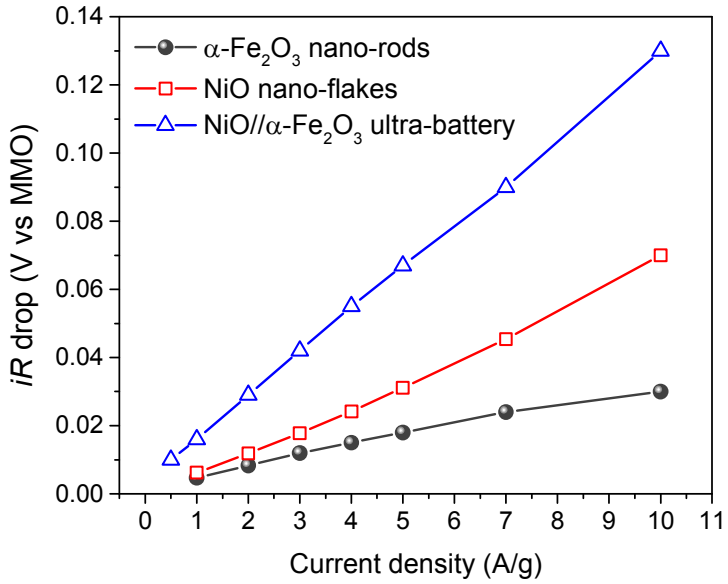

Figure S5. Plot of *iR*-drop values at different current densities for α-Fe_2O_3 nano-rod electrode, NiO nano-flake electrode and also for the assembled NiO//α-Fe_2O_3 ultra-battery.

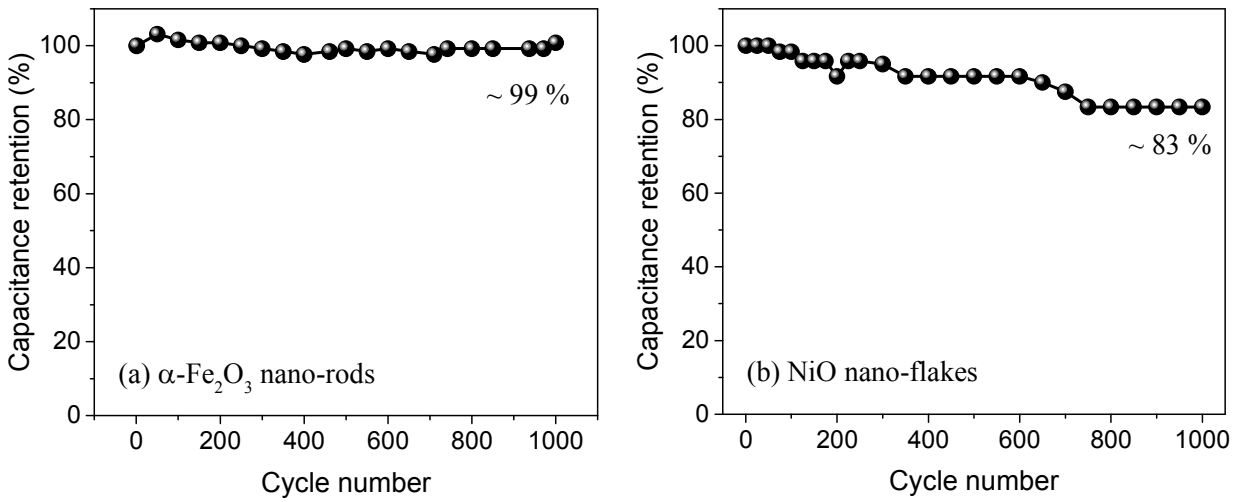

Figure S6. Cycling test for α-Fe_2O_3 nano-rod electrode (a) and NiO nano-flake electrode (b) at a current density of 1 A/g.

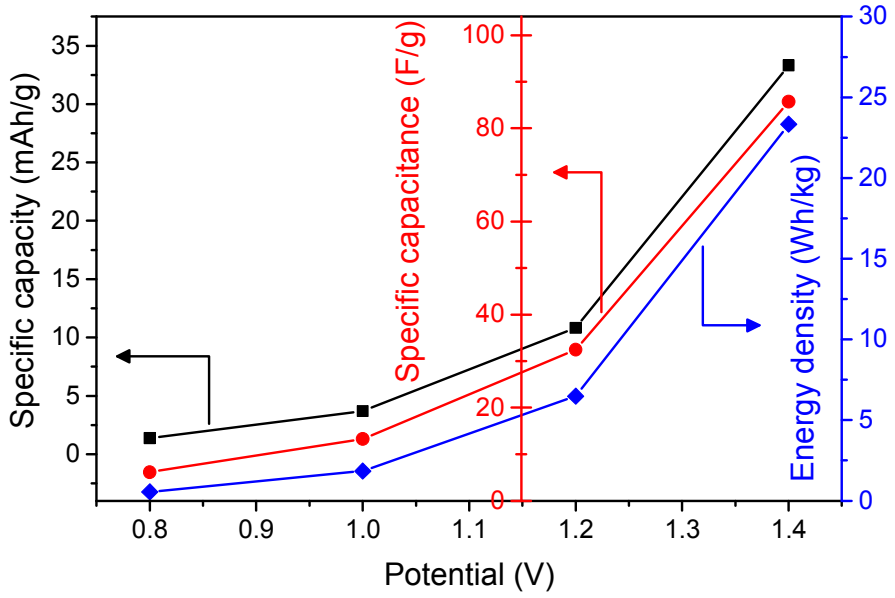

Figure S7. Specific capacitance, specific capacity and energy density for the NiO//α-Fe_2O_3 ultra-battery, calculated from the cyclic voltammetry curves at a scan rate of 50 mV/s as a function of potential window.

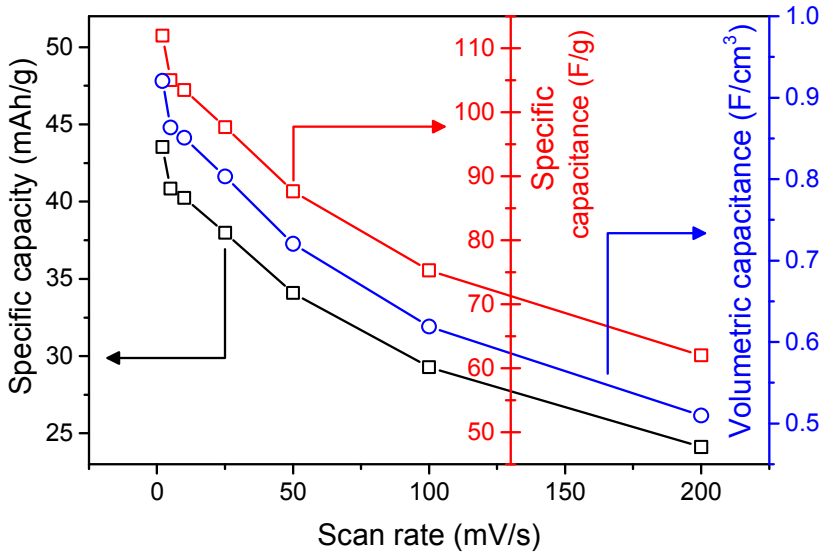

Figure S8. Plot of the specific capacity, specific capacitance and volumetric capacitances of the assembled NiO//α-Fe_2O_3 ultra-battery calculated from the CV loops at different potential scan rates.

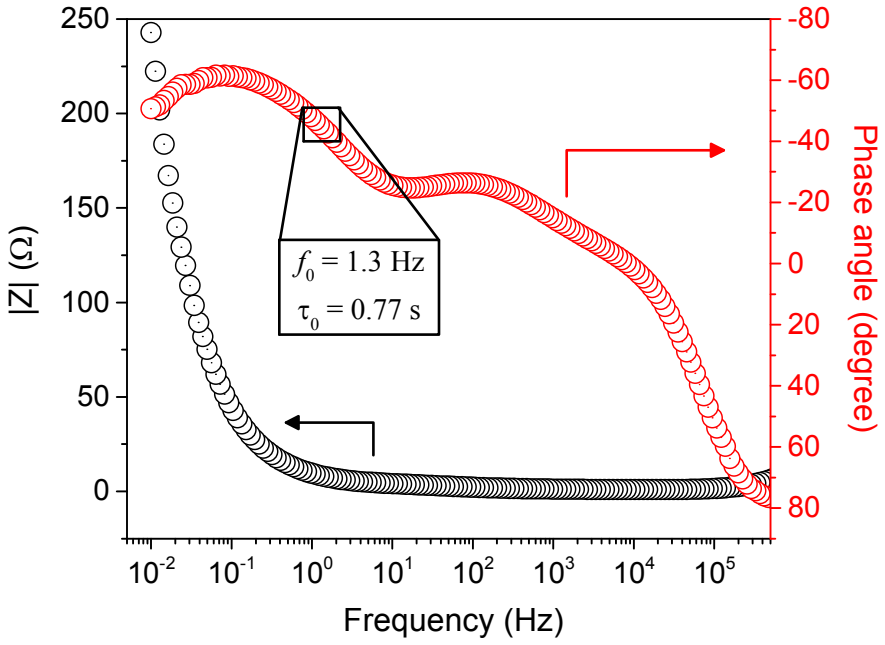

Figure S9. Bode plot of the assembled NiO//α-Fe_2O_3 ultra-battery within the frequency range of 10 mHz to 1 MHz with an AC field amplitude of 5 mV.

REFERENCES

(1) Vayssieres, L.; Sathe, C.; Butorin, S. M.; Shuh, D. K.; Nordgren, J.; Guo, J. One-Dimensional Quantum-Confinement Effect in α-Fe_2O_3 Ultrafine Nanorod Arrays. *Adv. Mater.* **2005**, *17*, 2320-2323.

(2) Kuiper, P.; Searle, B. G.; Rudolf, P.; Tjeng, L. H.; Chen, C. T. X-ray Magnetic Dichroism of Antiferromagnet Fe_2O_3: The Orientation of Magnetic Moments Observed by Fe 2p X-ray Absorption Spectroscopy . *Phys. Rev. Lett.* **1993**, *70*, 1549-1552.

(3) Shen, S.; Zhou, J.; Dong, C. L.; Hu, Y.; Tseng, E. N.; Guo, P.; Guo, L.; Mao, S. S. Surface Engineered Doping of Hematite Nanorod Arrays for Improved Photoelectrochemical Water Splitting. *Sci. Rep.* **2014**, *4*, 6627-6635.

(4) van der Laan, G.; Zaanen, J.; Sawatzky, G. A.; Karnatak, R.; Esteva, J.M. Comparison of X-ray Absorption with X-ray Photoemission of Nickel Dihalides and NiO. *Phys. Rev. B* **1986**, *33*, 4253-4263.

(5) Montoro, L. A.; Abbate, M.; Almeida, E. C.; Rosolen, J. M. Electronic Structure of the Transition Metal Ions in $LiCoO_2$, $LiNiO_2$ and $LiCo_{0.5}Ni_{0.5}O_2$. *Chem. Phys. Lett.* **1999**, *309*, 14-18.